

# Combustion and Detonation Waves in Gas Mixtures of CH<sub>4</sub>/Air, CH<sub>4</sub>/O<sub>2</sub>, and O<sub>2</sub>/Coal Dust

A. V. Pinaev<sup>a</sup> and P. A. Pinaev<sup>a</sup>

UDC 534.222.2 + 536.46 + 622.814

Published in *Fizika Goreniya i Vzryva*, Vol. 56, No. 6, pp. 56–68, November–December, 2020.  
Original article submitted December 18, 2019; revision submitted February 21, 2020; accepted for publication June 6, 2020.

**Abstract:** The combustion, explosion, and detonation in hybrid systems containing gas mixtures of CH<sub>4</sub>/air, CH<sub>4</sub>/O<sub>2</sub>, and O<sub>2</sub>/coal particles up to 200 μm in size with a volume-averaged density of up to 700 g/m<sup>3</sup> were studied on a vertical shock tube. X-ray diffraction patterns of the initial coal powder and coal samples subjected to high-temperature waves were analyzed. Data were obtained on the structure and parameters of waves in hybrid mixtures and in the same gas mixtures without coal dust. It is shown that in hybrid systems, coal dust has a weaker influence on the parameters of combustion and detonation waves than methane and that methane in these waves is more reactive than coal dust.

**Keywords:** methane, coal dust, mine explosions, combustion, detonation, explosion safety.

**DOI:** 10.1134/S0010508220060064

## INTRODUCTION

In the mining of coal, fine coal dust is deposited on the walls of the horizontal shaft. The air of the mine channel always contains airborne coal dust, whose concentration ( $\rho \leq 1$  g/m<sup>3</sup>) is 2–4 orders of magnitude lower than the lower concentration limit of explosiveness (30–80 g/m<sup>3</sup>) of coal dust [1–3]. Primary compression waves more commonly occur during explosions of methane–air mixtures near locations of accidental release of methane. Such a blast wave (shock wave (SW) with combustion products moving behind it) can entrain coal dust from the channel walls, produce a cloud of coal dust, and ignite it [1–5]. Combustion, explosion, and detonation of hybrid systems consisting of methane–air mixtures and coal dust are less studied than methane–air mixtures.

In experiments [5] under conditions close to those in mines, a channel section of length  $l$  and diameter  $d = 1$ –3 m was separated from the remaining longer

part of the channel using a thin paper or polyethylene partition and filled with methane. The methane–air mixture was fired with an igniter with an energy of several kilojoules. Usually,  $\Lambda = l/d \approx 3$ –20, and the blast wave did not have time to transform into detonation [5]. Behind the membrane, the channel section was covered with a coal dust layer, a binder inert solution was applied to a part of the coal dust surface, and explosion mitigation means were placed inside the channel [5–7]. Such studies are extremely time-consuming and costly.

The attenuation and initiation of blast and detonation waves (DWs) in dusty environments was investigated, e.g., in [8–22]. A chemical-kinetic method for preventing and extinguishing fires has been proposed [8, 9]. To provide explosion safety in a mine during dynamic processes, it is necessary to obtain data on the chemical activity of methane and coal dust [23]. To solve this problem, it is sufficient to compare the combustion and detonation wave parameters in methane-lean mixtures and in the same hybrid mixtures of methane with coal dust in shock-tube experiments, which are much less laborious than field tests. The purpose of this work was to obtain experimental data on

<sup>a</sup>Lavrent'ev Institute of Hydrodynamics, Siberian Branch,  
Russian Academy of Sciences, Novosibirsk, 630090  
Russia; avpin@ngs.ru.

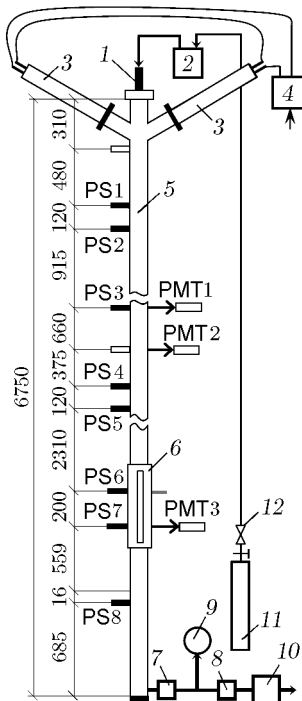


**Fig. 1.** Experimental setup: (1) dust generator; (2) container with coal powder; (3) initiation sections ( $d = 50$  mm and  $l_1 = 0.45$  m) with Mylar diaphragms; (4) high-voltage source; (5) shock tube test section ( $d = 70$  mm); (6) optical section; (7, 8) ball valves; (9) vacuum-pressure gauge; (10) backing pump; (11) 40-liters cylinder with a gas mixture; (12) reducer; the piezoelectric sensors are denoted as PS1–PS8 and photoelectron multipliers are denoted as PMT1–PMT3.

the parameters and structure of combustion and detonation waves in the above systems, starting from the moment of their ignition at different initiation energies.

## 1. EXPERIMENTAL SETUP AND PROCEDURE

The experiments were carried out in a vertical shock tube (Fig. 1) with dimensions  $l = 6.75$  m,  $d = 70$  mm, and  $\Lambda \approx 96$  at a temperature of 16–17°C. This value of  $\Lambda$  is usually sufficient for the establishment of the normal detonation mode. The tube was evacuated and filled with methane-lean (about 10% leaner) gas mixtures of CH<sub>4</sub>/O<sub>2</sub> and CH<sub>4</sub>/Air or oxygen or with the same gases with a coal suspension (hybrid mixtures) to an initial pressure  $p_0 = 0.025$ –0.1 MPa. Gas mixtures were fed from cylinder 11 through reducer 12. The hybrid mixture was produced by passing a gas mixture through container 2 with coal powder and through dust generator 1. The mass and volume-averaged concentra-

tion of coal dust particles in the tube was varied in the ranges  $m = 0.6$ –15.7 g and  $\rho = 23$ –700 g/m<sup>3</sup>. The self-ignition and combustion temperatures of coal were equal to 400 and 470°C, respectively.

Combustion and detonation waves were initiated by spark discharges with energy  $e_i \approx 1$  J from high-voltage source 4 (in this case, diaphragms between the sections were not placed) or with the aid of initiation sections (IS) (3) separated from the test section (TS) 5 by Mylar diaphragms. The ISs were filled with a mixture of C<sub>2</sub>H<sub>2</sub> + 2.5O<sub>2</sub> at an initial pressure  $p_{0i} = 0.05$ –0.36 MPa and initiated by spark discharges ( $e_i \approx 1$  J). During detonation combustion of the mixture, energy  $q_i \approx 15$ –106 kJ (specific initiation energy  $w_i = 4q_i/\pi d^2 \approx 3.8$ –27.6 MJ/m<sup>2</sup>) was released in the ISs, and the temperature of combustion products was  $\approx 4000$  K. In the upper section of the TS, the velocity of blast waves generated using ISs was 1000–1400 m/s.

During the initiation of the CH<sub>4</sub>/O<sub>2</sub> and CH<sub>4</sub>/O<sub>2</sub>/coal reactive systems using a spark or ISs, detonation propagates in the shock tube. In the experiments, detonation in these systems was initiated with the aid of ISs (see Section 3.1 below) since, in this case, the DW enters a steady-state mode faster than in the case of spark initiation. The reactivity of gas and hybrid systems was inferred from the parameters of steady-state detonation.

The less reactive mixtures of CH<sub>4</sub>/air and CH<sub>4</sub>/air/coal were initiated in two ways: using a spark and using ISs (see Section 3.2 below). During initiation by a spark, a combustion wave propagates in the shock tube, and during initiation of the same systems by ISs, attenuating blast waves propagate.

Luminescence and pressure profiles in compression waves were recorded by three 4-beam Tektronix TDS2014 oscilloscopes, signals to which were fed from photoelectron multipliers (PMT1–PMT3) and piezoelectric sensors (PS1–PS8) through source-follower amplifiers with a time constant of 0.5–2 s. The natural frequency of the piezoelectric sensors was 300 kHz, and the design and calibration methods of the sensors are described in [24–26]. The measurement error for pressure did not exceed 5%, and for wave velocity, it was 1%.

## 2. COAL POWDER

The initial blocks (<1 cm) of Kuzbass coal were crushed in a tumbling machine with steel balls 10–40 mm in diameter for 2 h. Particles larger than 0.5 mm were removed using a sieve with a mesh size of 500  $\mu$ m. From 100 g of a powder fraction of 0–500  $\mu$ m through 200, 140, and 94  $\mu$ m mesh sieves, fractions of

500–200, 200–140, 140–94, and 0–94  $\mu$ , weighing 41, 15, 20, 16 g respectively, were obtained. The residual powder fraction on the sieves weighed 8 g and had a particle size of 0–10  $\mu$ m. Their mass fraction can be determined from the mass of coal powder fractions. Powder fractions and the sieves were weighed on a balance with an error of 0.1 g and examined under a microscope.

Particles less than 10  $\mu$ m are not sifted into the residue and are always present among large particles and on the sieves; therefore the real proportion of particles in the fractions is lower than the specified values. The mass percentage of the obtained fractions with sizes less than 200  $\mu$ m is low, and the process of screening out these fractions is laborious. For these reasons, from a powder fraction of 0–500  $\mu$ m sieved through a 200  $\mu$ m mesh sieve, fractions of 200–500 and 0–200  $\mu$ m were obtained. The experiments were carried out with a coal powder of 0–200  $\mu$ m; this fraction has poor flowability and is prone to agglomeration due to the binder fine fraction. Dust generator 1 ensured uniform supply of this fraction into the tube, as was established by weighing the coal powder in container 2 (Fig. 1) at different times. Images and the elemental composition of coal and impurity particles were obtained on a Merlin Compact, Zeiss scanning electron microscope. Impurity particles in the images have characteristic luster.

The main elements of coal are C, O, Si, Al, Ca, and S (average mass content 78.35, 19.75, 0.69, 0.41, 0.25, and 0.16%, respectively), and the main impurity elements are C, O, Si, Al, Fe, Ca, and Mg (25.08, 39.06, 13.33, 8.41, 7.79, 2.69, and 1.95%, respectively). In the impurity, the percentage of C is lower and the percentages of O, Si, Al, Fe, Ca, and Mg are higher than in coal.

The chemical composition of the crystalline substances of coal and impurity particles was determined on a D8-Advance X-ray diffractometer (radiation Cu  $K_\alpha$ ). For the coal, the crystalline carbon lines are absent, and in the vicinity of an angle of 26°C there is a wide halo corresponding to amorphous carbon. In impurity particles, crystalline substances correspond to the lines of quartz ( $\text{SiO}_2$ ) and the closely spaced lines of kaolinite  $\text{Al}_4[\text{Si}_4\text{O}_{10}](\text{OH})_8$  and chlorite  $(\text{Mg,Fe,Al})_6(\text{Al,Si})_4\text{O}_{10}(\text{OH})_8$ , which are clay components, the clay is dominated by kaolinite.

### 3. EXPERIMENTAL RESULTS

#### 3.1. Detonation of Mixtures of $\text{CH}_4 + 11.346\text{O}_2$ and $(\text{CH}_4 + 11.346\text{O}_2)/\text{Coal}$ in the Test Section

3.1.1.  $p_0 = 0.1$  MPa. (A) For the fuel-lean mixture of  $\text{CH}_4 + 11.346\text{O}_2$ , the calculated detonation velocity

is  $D_0 \approx 1640$  m/s, and the effective length of the reaction zone (detonation cell size)  $a \approx 30$  mm [27]. After the detonation combustion of the mixture of  $\text{C}_2\text{H}_2 + 2.5\text{O}_2$  in the IS at  $p_{0i} = 0.15$  MPa ( $w_i \approx 11.5$  MJ/m<sup>2</sup>) and diaphragm rupture, an accelerating DW is initiated in the gas mixture under study. The DW velocities at the bases of PS1–PS8 are  $D_{12} \approx 1200$ ,  $D_{24} \approx 1182$ ,  $D_{34} \approx 1170$ ,  $D_{45} \approx 1263$ ,  $D_{67} \approx 1626$ , and  $D_{78} \approx 1600$  m/s. In the lower part of the tube, the DW enters the normal detonation mode, and the sensors record a pressure drop in the reaction zone (characteristic von Neumann spike) behind the shock front.

After reflection of the detonation wave, a SW propagates from the lower end of the tube upward. Here and in further experiments, due to a change in the particle velocity and the counter-flow pressure, the reflected SW velocity increases ( $D_{87} \approx 927$  and  $D_{76} \approx 952$  m/s).

At a higher initiation energy ( $p_{0i} = 0.2$  MPa and  $w_i \approx 15.3$  MJ/m<sup>2</sup>), the DW propagates almost steadily:  $D_{12} \approx 1714$ ,  $D_{24} \approx 1612$ ,  $D_{34} \approx 1592$ ,  $D_{45} \approx 1600$ ,  $D_{67} \approx 1570$ , and  $D_{78} \approx 1562$  m/s. The reflected SW velocities are  $D_{87} \approx 767$  and  $D_{76} \approx 816$  m/s. Figure 2a shows typical oscillograms of pressure and luminescence in the lower part of the tube for this experiment. Here and below, the pressure jump along the vertical for the sensors is  $\Delta p = p - p_0$ .

(B) For stoichiometry, it is necessary to add 10.6 g of carbon to the mixture of  $\text{CH}_4 + 11.346\text{O}_2$  in the TS at  $p_0 = 0.1$  MPa; the result is a stoichiometric mixture of  $\text{CH}_4 + 11.346\text{O}_2 + 9.346\text{C}$ . This amount of carbon corresponds to a mass of coal suspension  $m \approx 13.5$  g ( $\rho \approx 603$  g/m<sup>3</sup>). Experiments with hybrid systems were performed in the range  $27 \leq \rho \leq 260$  mg/m<sup>3</sup>.

At  $p_{0i} = 0.15$  MPa, in the hybrid mixture of  $(\text{CH}_4 + 11.346\text{O}_2)/\text{coal}$ ,  $\rho \approx 190$  g/m<sup>3</sup>, unlike in the gas mixture, the DW acquires an almost steady-state velocity already in the initial section of the tube:  $D_{12} \approx 1714$ ,  $D_{24} \approx 1639$ ,  $D_{34} \approx 1617$ ,  $D_{45} \approx 1714$ , and  $D_{67} \approx D_{78} \approx 1575$  m/s. The velocities of the shock wave reflected from the end face are  $D_{87} \approx 927$  and  $D_{76} \approx 952$  m/s. Due to the ignition and combustion of coal particles, the luminescence in the wave becomes more intense and lasting. Due to incomplete combustion, the coal suspension behaves as a chemically inert medium: the momentum is lost in the DW, and the detonation velocity at the end of the tube becomes about 20 m/s lower than in the gas mixture.

In the case of stronger initiation ( $p_{0i} = 0.20$  MPa,  $w_i \approx 15.3$  MJ/m<sup>2</sup>) and  $\rho \approx 248$ –260 g/m<sup>3</sup>, the DW also propagates almost steadily:  $D_{12} \approx 1670 \pm 5$ ,  $D_{24} \approx 1652 \pm 20$ ,  $D_{45} \approx 1656 \pm 13$ ,  $D_{67} \approx 1614 \pm 5$ , and  $D_{78} \approx 1633 \pm 10$  m/s. The luminescence on the “plateau” in the wave (duration >3 ms) increases in in-

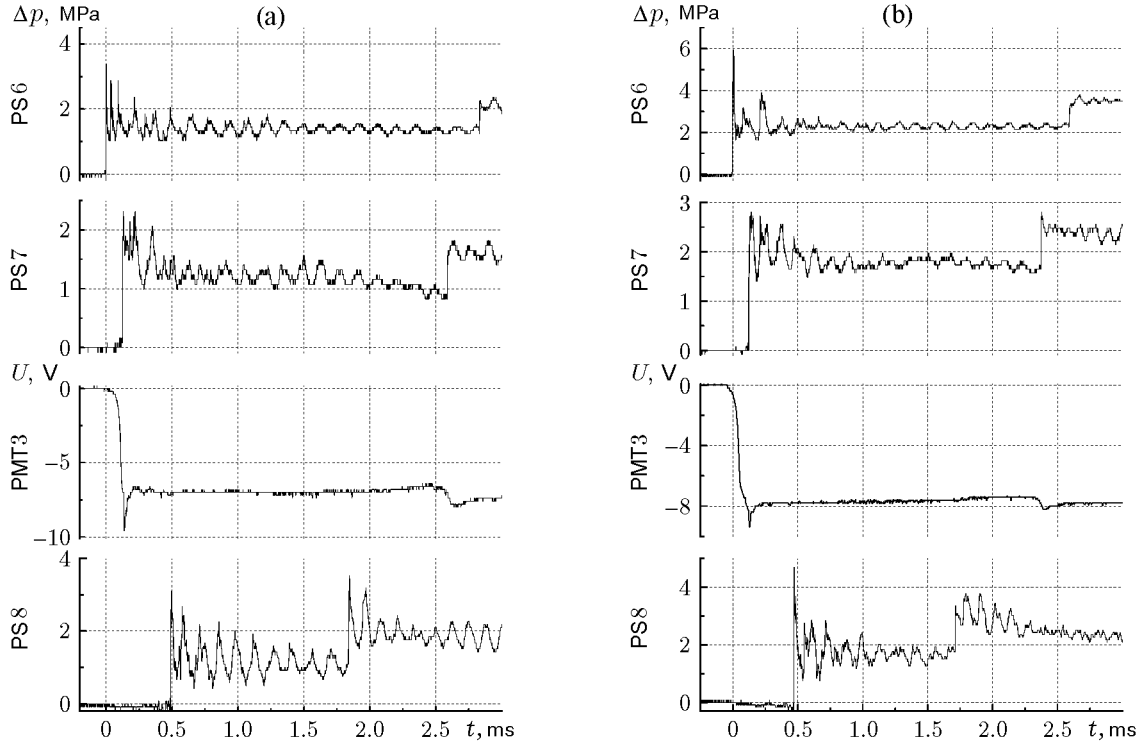


**Fig. 2.** Oscillograms of pressure and luminescence in the DW ( $p_0 = 0.1$  MPa,  $p_{0i} = 0.2$  MPa, and  $w_i \approx 15.3$  MJ/m<sup>2</sup>): (a) gas mixture of CH<sub>4</sub> + 11.346O<sub>2</sub>; (b) hybrid mixture of (CH<sub>4</sub> + 11.346O<sub>2</sub>)/coal ( $\rho \approx 260$  g/m<sup>3</sup>,  $D_{12} \approx 1667$ ,  $D_{24} \approx 1681$ ,  $D_{34} \approx 1669$ ,  $D_{45} \approx 1622$ ,  $D_{67} \approx 1613$ , and  $D_{78} \approx 1643$  m/s).

tensity by about 12% compared to the luminescence in the gas mixture (Fig. 2b). The reflected SW velocities are  $D_{87} \approx 849 \pm 20$  and  $D_{76} \approx 909 \pm 5$  m/s.

Due to the deceleration of the gas flow on coal particles, the pressure at the DW front in the hybrid mixture at  $\rho \approx 190$  g/m<sup>3</sup> increases by 14–20 % and at  $\rho \approx 248$ –260 g/m<sup>3</sup>, by 30–70% compared to the pressure in the DW front in the gas mixture of CH<sub>4</sub> + 11.346O<sub>2</sub>.

It follows from our experiments that combustion of coal particles begins in the reaction zone ( $a \approx 30$  mm) and continues behind it. However, the resulting heat release in the reaction zone practically does not change compared to the gas mixture, and the detonation velocity does not increase. After DW reflection from the end face, a SW propagates upward. According to the results of electron microscopic measurements of spectra, the concentration of elements on a coal particle before and after the experiments are close to each other and are within the range of data variation.

After the experiments, there is an increase in the percentage of ideally spherical impurity particles ranging in size from fractions to tens of micrometers (Fig. 3). These particles have time to be heated in the detonation wave and melted, after which they take a spherical

shape due to surface tension forces and keep it during cooling. Similar spherical particles are observed in the experiments described below.

**3.1.2.  $p_0 = 0.025$  MPa.** (A) To elucidate the effect of the length of the reaction zone on the detonation parameters and the degree of burnout of coal particles, we performed experiments at reduced initial pressures in the TS. Detonation in the gas mixture of CH<sub>4</sub> + 11.346O<sub>2</sub> was initiated in the same manner as in the experiments at  $p_{0i} = 0.1$  MPa (see Section 3.1.1). The luminescence behind the front of the passing DW in the lower part of the tube lasts approximately 1.5 ms, which corresponds to an area of 2.3 m (see PMT3 Fig. 4a); here  $a \approx 120$  mm at  $p_0 = 0.025$  MPa (increases in inverse proportion to  $p_0$ ). The detonation wave propagates in the spin mode with a frequency of rotation of the “head”  $f \approx 7.41$  kHz (PS6–PS8 in Fig. 4a). From this frequency, using the relation  $c = \pi df / 1.84$  [28], we can estimate the speed of sound in the detonation products:  $c_1 \approx 886$  m/s. The DW velocities along the length are  $D_{12} \approx 1463$ ,  $D_{24} \approx 1632$ ,  $D_{34} \approx 1617$ ,  $D_{45} \approx 1579$ ,  $D_{67} \approx 1538$ , and  $D_{78} \approx 1554$  m/s. In the reflected SW (velocities  $D_{87} \approx 710$  and  $D_{76} \approx 724$  m/s), the luminescence is enhanced (PMT3 in Fig. 4a).

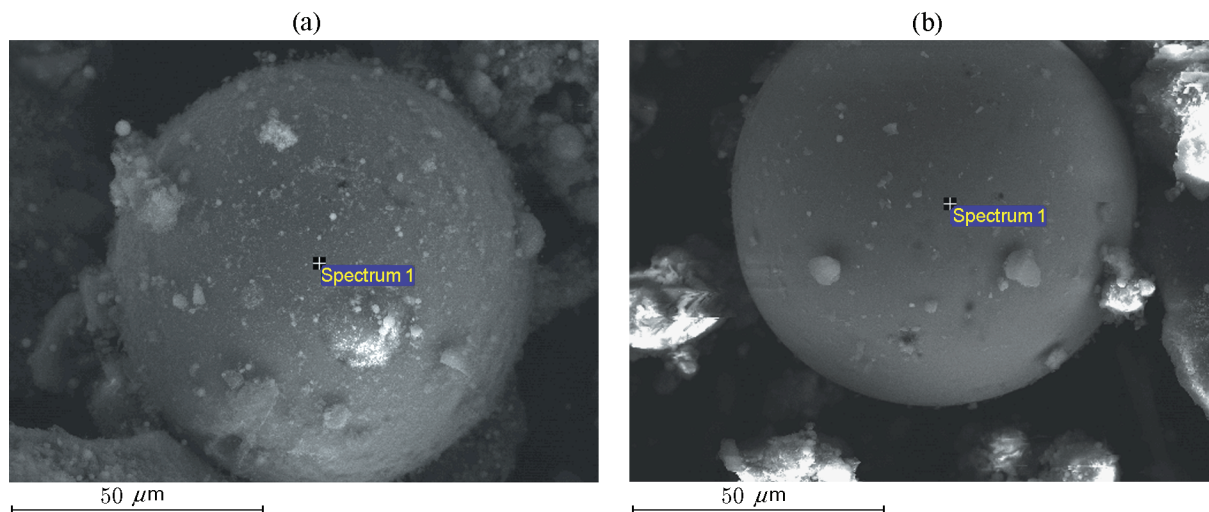


**Fig. 3.** Hybrid mixture of  $(\text{CH}_4 + 11.346\text{O}_2)/\text{coal}$ : large ( $80\text{--}85\ \mu\text{m}$ ) and small ( $1\text{--}2\ \mu\text{m}$ ) spherical impurity particles in coal that are formed after exposure to the DW for  $\rho \approx 190$  (a) and  $260\ \text{g/m}^3$  (b), respectively.

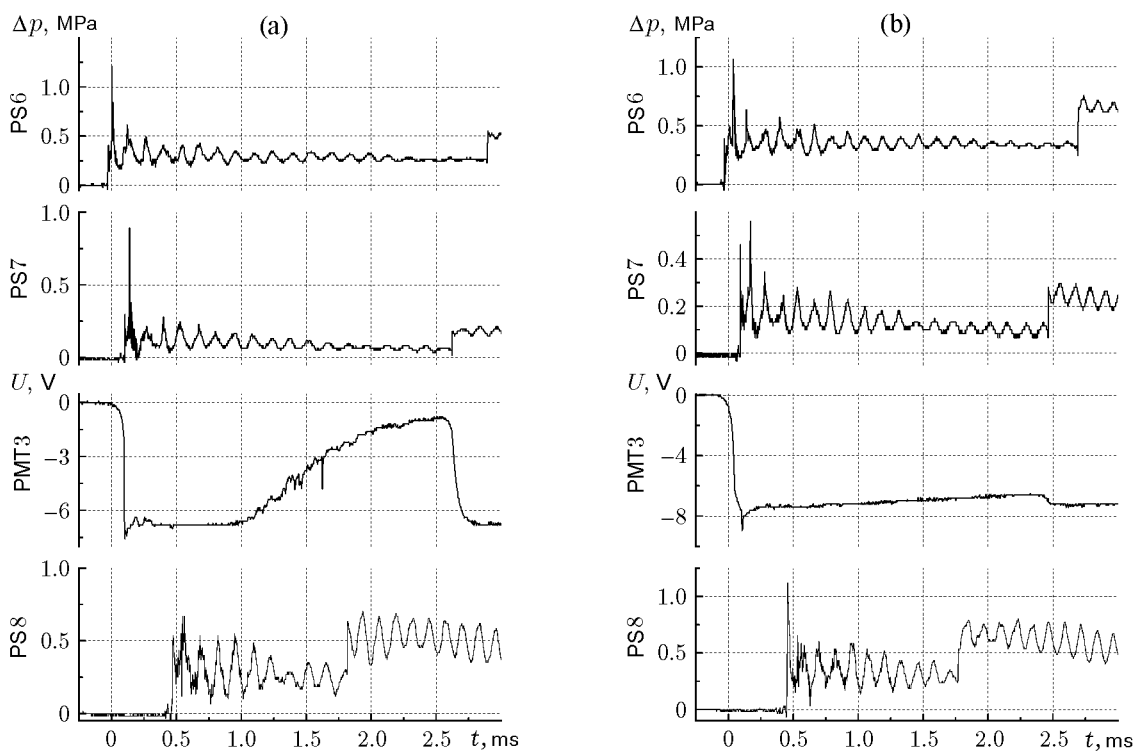


**Fig. 4.** Oscillograms of pressure and luminescence in the DW ( $p_0 = 0.025\ \text{MPa}$ ,  $p_{0i} = 0.1\ \text{MPa}$ , and  $w_i \approx 7.7\ \text{MJ/m}^2$ ): (a)  $\text{CH}_4 + 11.346\text{O}_2$ ; (b)  $(\text{CH}_4 + 11.346\text{O}_2)/\text{coal}$  ( $\rho \approx 80\ \text{g/m}^3$ ).

(B) In the case of the same initiation of the hybrid mixture in the DW, the luminescence in the reaction zone and behind is higher than in the gas mixture, due to the combustion of coal particles, resulting in an increase in the burning time and the merging of

the intensity signals in the incident and reflected waves (PMT3 in Fig. 4b). Here the DW front velocities are  $D_{12} \approx 1714$ ,  $D_{24} \approx 1667$ ,  $D_{34} \approx 1669$ ,  $D_{45} \approx 1710$ ,  $D_{67} \approx 1538$ , and  $D_{78} \approx 1554\ \text{m/s}$ , the reflected SW velocities are  $D_{87} \approx 821$  and  $D_{76} \approx 870\ \text{m/s}$ . The deto-

nation wave enters a single-head spin mode with a rotation frequency  $f \approx 7.94$  kHz (PS6–PS8 in Fig. 4b), and the speed of sound in the detonation products is  $c_2 \approx 949$  m/s. At the end of the tube, the DW velocity increases by 40 m/s. The temperature behind the reaction zone in the hybrid mixture  $T_2 \approx T_1 \sqrt{c_2/c_1} \approx 1.15T_1$  is about 15% higher than the temperature  $T_1$  during detonation of the same gas mixture.

On coal particles and impurity particles, the concentrations of elements before the experiment and after the DW passage are within the range of data variation.

### 3.2. Combustion and Explosion in CH<sub>4</sub>/Air Gas System and CH<sub>4</sub>/Air/Coal Hybrid System

**3.2.1. Combustion in the Initiation Section and in the Test Section.** (A) The test section and the initiation sections are filled with a mixture of CH<sub>4</sub> + 10.52 air, there are no diaphragms in the tube, and initiation was carried out by a spark with energy  $e_i \approx 1$  J. The calculated detonation parameters for the gas mixture of CH<sub>4</sub> + 10.52 air at  $p_0 = 0.1$  MPa are  $D_0 = 1770$  m/s and  $a \approx 260$  mm, and the pressure in the Chapman–Jouguet plane is  $p_{CJ} = 1.66$  MPa [27]. This mixture is about 10% leaner in methane than the stoichiometric methane–air mixture of CH<sub>4</sub> + 9.524 air. In a tube with a diameter  $d = 70$  mm, steady-state detonation does not propagate even in the spin mode since  $\pi d < a$ .

At  $p_0 = 0.05$  MPa, the mixture is not initiated by a spark. With an increase in pressure to  $p_0 = 0.085$  MPa, the flame begins to propagate in the tube in a near-limit mode. At  $p_0 = 0.1$  MPa, the flame moves steadily in the tube, and the compression waves overtake the flame front. The luminescence in the combustion wave is weak and lasts approximately 70–200 ms. The flame front velocities are  $D_{24} \approx 325$ ,  $D_{34} \approx 260$ ,  $D_{45} \approx 120$ ,  $D_{67} \approx 0.91$ – $1.25$ , and  $D_{78} \approx 1.44$  m/s; there is no reflected wave.

(B) In the hybrid mixture of (CH<sub>4</sub> + 10.52 air)/coal ( $\rho \approx 100$ – $546$  g/m<sup>3</sup>) under the same experimental conditions and  $p_0 = 0.1$  MPa, the luminescence intensity in the combustion wave increases by more than an order of magnitude, and the compression waves at the end of the tube become steeper than in the gas mixture. The flame front velocities are  $D_{24} \approx 13$ ,  $D_{34} \approx 10$ – $13$ ,  $D_{67} \approx 1.43$ – $1.82$ , and  $D_{78} \approx 1.15$ – $1.37$  m/s. In the hybrid mixture, the flame velocity at the top of the tube is lower than in the similar gas mixture.

According to electron microscopic measurements of spectra, the concentration of elements on coal particles before and after the experiments are within the data variation range.

### 3.2.2. Blast Waves in the Test Section ( $p_0 = 0.1$ MPa).

(A) The gas mixture of CH<sub>4</sub> + 10.52 air at  $p_0 = 0.1$  MPa in the TS was initiated with the aid of an IS filled with a mixture of C<sub>2</sub>H<sub>2</sub> + 2.5O<sub>2</sub> at  $p_{0i} = 0.1$  MPa. Under this more powerful initiation than that in Section 3.2.1, an attenuating blast wave propagates in the TS. Between PMT1 and the PMT2, the flame front velocity is 600 m/s, and the luminescence in this section lags behind the SW front by 450  $\mu$ s. On the PMT3 at the bottom of the tube, the flame lags behind the SW front already by 4 ms. The blast wave front velocities are  $D_{12} = 1000$ – $1043$ ,  $D_{24} = 878$ – $886$ ,  $D_{34} = 835$ – $885$ ,  $D_{45} = 828$ – $857$ ,  $D_{67} = 769$ – $810$ , and  $D_{78} = 767$ – $788$  m/s. In the reflected wave propagating in the hot gas, steady-state low-velocity detonation occurs:  $D_{87} \approx 1265$ – $1515$ ,  $D_{76} \approx 1290$ – $2000$ ,  $D_{54} \approx 1200$ – $2000$ ,  $D_{43} \approx 1150$ – $1620$ ,  $D_{42} \approx 1170$ – $1575$ , and  $D_{21} \approx 1200$ – $1500$  m/s. The beginning of the DW luminescence almost coincides with the leading shock front of the wave.

With an increase in the initiation power ( $p_{0i} = 0.2$  MPa and  $w_i \approx 15.3$  MJ/m<sup>2</sup>) at  $p_0 = 0.1$  MPa, a stronger blast wave propagates in the shock tube:  $D_{12} = 1200$ – $1333$ ,  $D_{24} = 1083$ – $1178$ ,  $D_{34} \approx 1035$ – $1089$ ,  $D_{45} = 1043$ – $1091$ ,  $D_{67} = 910$ – $930$ , and  $D_{78} = 905$ – $927$  m/s. As in the case  $p_{0i} = 0.1$  MPa, the gas mixture does not burn completely, and in the reflected wave in the lower part of the tube (Fig. 5a), low-velocity detonation occurs with the velocities  $D_{87} \approx 1369$ – $1513$  and  $D_{76} \approx 1429$ – $1600$  m/s and luminescence in the front. In the upper part of the tube, the low-velocity DW propagates at approximately constant velocity:  $D_{54} \approx 1412$ – $1145$ ,  $D_{43} \approx 1362$ – $1669$ ,  $D_{42} \approx 1445$ – $1696$ , and  $D_{21} \approx 1470$ – $1500$  m/s.

(B) The hybrid mixture of (CH<sub>4</sub> + 10.52 air)/coal was initiated, as above, with the aid of ISs using a gas mixture of C<sub>2</sub>H<sub>2</sub> + 2.5O<sub>2</sub>. Under the initial conditions ( $p_{0i} = 0.1$  MPa and  $p_0 = 0.1$  MPa), luminescence behind the blast wave in the hybrid mixture of (CH<sub>4</sub> + 10.52 air)/coal ( $\rho \approx 23$ – $230$  g/m<sup>3</sup>) increases by more than an order of magnitude compared to the previous case, due to the combustion of coal particles. However, since in the upper part of the tube, the flame detaches from the leading shock front by about 0.3 m, and coal combustion starts in the initial flame region. Due to the significant lag of the reaction zone behind the shock front, the wave is not accelerated. The wave front velocities along the length in the hybrid mixture are lower than in the similar gas mixture:  $D_{12} \approx 1000$ – $1200$ ,  $D_{24} \approx 882$ – $942$ ,  $D_{34} \approx 841$ – $885$ ,  $D_{45} \approx 857$ – $889$ ,  $D_{67} \approx 769$ – $909$ , and  $D_{78} \approx 757$ – $772$  m/s. The detachment of the flame from the front increases with distance, but behind the leading shock front at the bottom of the tube,

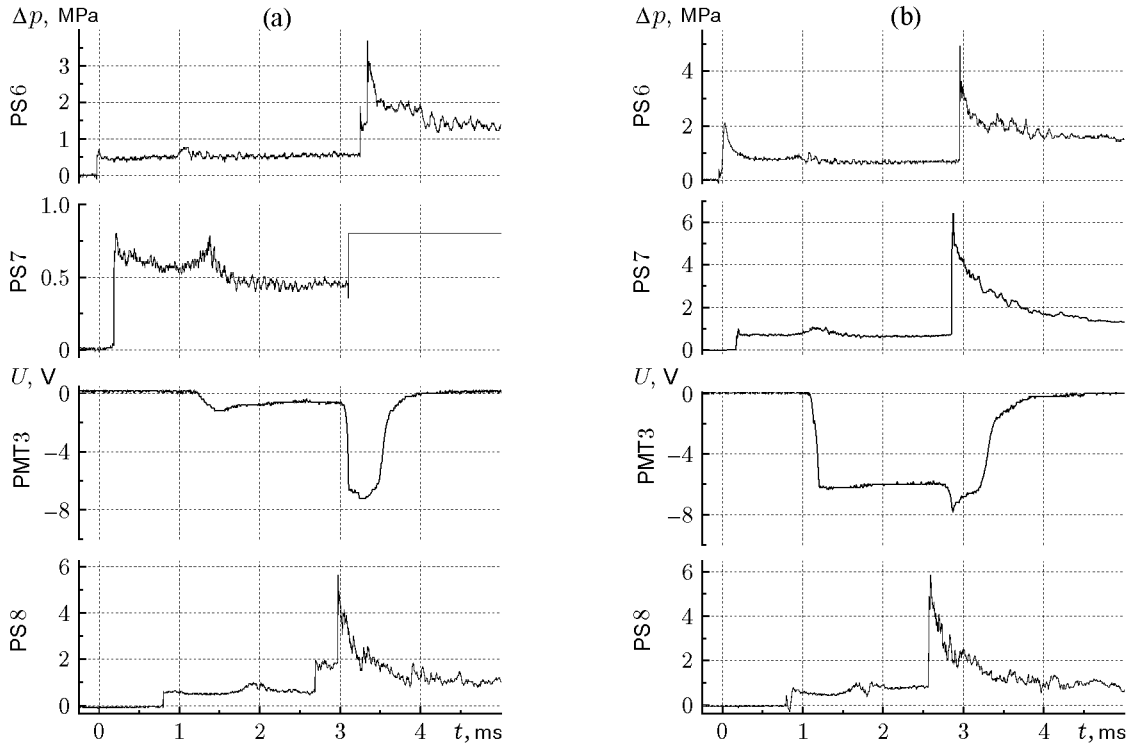


**Fig. 5.** Oscillograms of pressure and luminescence ( $p_0 = 0.1$  MPa): (a)  $\text{CH}_4 + 10.52$  air ( $p_{0i} = 0.2$  MPa); (b)  $(\text{CH}_4 + 10.52 \text{ air})/\text{coal}$  ( $p_{0i} = 0.2$  MPa and  $\rho \approx 530 \text{ g/m}^3$ ).

a flat compression wave is formed with a powerful luminescence in it. This compression wave moves to the leading front and meets the wave reflected from the end of the tube. In fact, the reflected wave is a low-velocity DW and propagates from bottom to top at a velocity lower than in the gas mixture:  $D_{87} \approx 1322\text{--}1337$ ,  $D_{76} \approx 1333\text{--}1429$ ,  $D_{54} \approx 1263\text{--}1333$ ,  $D_{42} \approx 1193\text{--}1423$ , and  $D_{21} \approx 1333\text{--}942$  m/s.

Under more powerful initiation ( $p_{0i} = 0.2$  MPa), qualitative and quantitative changes occur in the hybrid mixture ( $\rho \approx 8\text{--}530 \text{ g/m}^3$ ), and the luminescence sharply increases behind the wave front (see Fig. 5b). The blast wave is also attenuating, but the wave velocities increase in comparison with the case of initiation at  $p_{0i} = 0.1$  MPa:  $D_{12} \approx 1200\text{--}1333$ ,  $D_{24} \approx 1054\text{--}1089$ ,  $D_{34} \approx 1005\text{--}1089$ ,  $D_{45} \approx 1000\text{--}1091$ ,  $D_{67} \approx 901\text{--}917$ , and  $D_{78} \approx 885\text{--}927$  m/s.

In the lower part of the tube, a compression wave with luminescence is formed behind the SW front. The reflected wave is a detonation wave and propagates with a higher velocity than at  $p_{0i} = 0.1$  MPa:  $D_{87} \approx 1513\text{--}1983$  and  $D_{76} \approx 1429\text{--}2000$  m/s, and powerful luminescence is observed in the front of the reflected DW. In the upper part of the tube, the DW velocities are  $D_{54} \approx 1412\text{--}1500$ ,  $D_{43} \approx 1522\text{--}1630$ ,  $D_{42} \approx$

$1444\text{--}1696$ , and  $D_{21} \approx 1500\text{--}1520$  m/s. Here the lower reflected wave velocities corresponds to the lowest concentration of the coal suspension ( $\rho \approx 8 \text{ g/m}^3$ ). At such a low concentration, the parameters of the incident and reflected waves are determined by the gas mixture of  $\text{CH}_4 + 10.52$  air.

The coal mixture burns in the incident and reflected detonation waves from the lower end of the tube. The parameters of the second reflected wave propagating from top to bottom of the tube at  $\rho \approx 23\text{--}230 \text{ g/m}^3$  and  $p_{0i} = 0.1$  MPa are  $D_{12} \approx 1714\text{--}2014$ ,  $D_{67} \approx 1797\text{--}1982$ , and  $D_{78} \approx 1818\text{--}2000$  m/s. The second reflected wave at  $\rho \geq 23 \text{ g/m}^3$  is also a detonation wave; it is maintained by the combustion reaction of coal particles. However, at  $\rho \approx 8 \text{ g/m}^3$ , the coal suspension has little effect on the velocity of the second reflected wave:  $D_{12} \approx 860$  and  $D_{24} \approx 890$  m/s, which correspond to SWs without energy release.

The parameters of the first blast wave in the gas and hybrid mixtures increase with increasing initiation energy. In all experiments with coal suspensions at  $\rho \geq 23 \text{ g/m}^3$ , the reflected DW velocity is  $400\text{--}600$  m/s higher than in the similar gas mixture under the same initial conditions. The first and second reflected waves are detonation waves. In hybrid mixtures, a significant

part of the coal settles on the bottom flange and partial combustion of coal is observed. The percentage of burned coal is usually not higher than 20–30% and depends on the value of  $\rho$ .

Our experiments show that relatively short-time combustion of fine coal in combustion, blast, and detonation waves, is inferior in efficiency to the longer-time method of burning coal in boilers and furnaces.

### 3.3. Low-Velocity Detonation of a Mixture of (CH<sub>4</sub> + 2O<sub>2</sub> + 6N<sub>2</sub>)/Coal in the Test Section

(A) In a gas mixture of CH<sub>4</sub> + 2O<sub>2</sub> + 6N<sub>2</sub>, the fuel and oxidizer are in a stoichiometric ratio, and the calculated Chapman–Jouguet detonation parameters are  $D_0 = 1867$  m/s and  $a \approx 83$  mm [27]. This mixture is interesting in that its detonation parameters are close to the detonation parameters of the mixture of CH<sub>4</sub> + 11.346O<sub>2</sub> (see Section 3.1), but the mixture of CH<sub>4</sub> + 2O<sub>2</sub> + 6N<sub>2</sub> does not contain free (excessive) oxygen. This allows a direct comparison of the reactivity of methane and coal dust in the hybrid system. The mixture was initiated with the aid of ISs filled with a mixture of C<sub>2</sub>H<sub>2</sub> + 2.5O<sub>2</sub>. In the experiments, we determined the optimal initial pressure  $p_{0i} = 0.25$  MPa in the ISs at which the DW propagates almost steadily throughout the tube:  $D_{12} \approx 1765$ –1935,  $D_{24} \approx 1848$ –1857,  $D_{34} \approx 1822$ –1848,  $D_{45} \approx 1714$ –1875,  $D_{67} \approx 1818$ –1852, and  $D_{78} \approx 1831$ –1855 m/s. The pressure profiles in the DW have a characteristic von Neumann spike: a jump in the shock front and a subsequent almost twofold reduction in pressure at the end of the reaction zone (Fig. 6a). The start of the luminescence signal almost coincides with the shock front. The length of the reaction zone measured experimentally from pressure profiles is 37–56 mm. The frequency of luminescence and pressure pulsations in the DW is  $f \approx 7.81$ –8.13 kHz. The reflected wave is a SW with a rectangular pressure profile and with  $D_{87} \approx 871$ –878 and  $D_{76} \approx 909$ –917 m/s (Fig. 6a).

(B) From the above experiments with hybrid mixtures, it follows that methane is chemically more active and burns faster than the coal suspension, and, therefore, it is logical to expect that in the mixture of (CH<sub>4</sub> + 2O<sub>2</sub> + 6N<sub>2</sub>)/coal, the coal suspension will behave as the inert curtain studied in [10, 11]. However, the experimental results were not quite unambiguous.

In the experiments, the following pattern was observed. If the DW velocity at the end of the tube decreased to about 1300–1500 m/s, the reflected wave was also a low-velocity detonation wave with a von Neumann spike and propagated at about the same velocity  $D_{87} \approx 1495$ –1370 m/s and  $D_{76} \approx 1470$ –1430 m/s

(Fig. 6b). However, if the wave attenuated even more significantly, to  $D_{78} \approx 1100$  m/s ( $\rho \approx 515$  g/m<sup>3</sup>), then, after its reflection, a strong DW with a von Neumann spike ( $D_{87} \approx 1898$  and  $D_{76} \approx 1818$  m/s) was initiated (Fig. 6c). In this case, the beginning of the luminescence zone in the reflected wave almost coincided with the leading detonation front. In the incident DW at the end of the tube, the reaction zone is 150–500  $\mu$ s (20–55 cm) ahead of the leading front, the pressure profile near the leading front is unstable, and the pressure at the initial region of the luminescent flame zone increases smoothly (Figs. 6 and 6c).

For the same parameters of the initiating source as in Section 3.3 (A) ( $p_{0i} = 0.25$  MPa and  $w_i \approx 19.2$  MJ/m<sup>2</sup>) and for  $\rho \approx 179$ –515 g/m<sup>3</sup>, the detonation velocity in the initial section ( $x \leq 0.85$  m) is 270–430 m/s lower than in the gas mixture (Fig. 7). At  $x \approx 2.3$  m, the wave velocity decreases to  $D \approx 1150$ –1300 m/s. If  $\rho < 500$  g/m<sup>3</sup>, then on a length of  $2.3 \text{ m} < x \leq 3$  m, the DW velocity increases by 50–350 m/s, but then decreases again to the coordinate  $x \approx 4.8$  m. After  $x > 4.8$  m, the wave velocity increases by 30–100 m/s. The wave velocities along the tube length at  $p_{0i} = 0.25$  MPa and  $\rho \approx 179$ –515 g/m<sup>3</sup> are  $D_{12} \approx 1500$ –1510,  $D_{24} \approx 1345$ –1219,  $D_{34} \approx 1294$ –1150,  $D_{45} \approx 1333$ –1142,  $D_{67} \approx 1266$ –1111, and  $D_{78} \approx 1369$ –1095 m/s. If the density of the coal suspension increases to  $\rho \approx 515$  g/m<sup>3</sup>, the DW velocity decreases monotonically along the tube length from  $D_{12} \approx 1500$  m/s to  $D_{78} \approx 1100$  m/s (see Fig. 7).

Thus, the coal dust attenuates the DW in the gas stoichiometric mixture, and the reflection of the wave leads to the initiation of low-velocity or high-velocity detonation, depending on the degree of attenuation of the incident wave. It is possible that at suspension densities  $\rho > 500$  g/m<sup>3</sup>, the coal suspension will attenuate the wave up to complete suppression of the DW.

### 3.4. Blast Waves in the O<sub>2</sub>/Coal Mixture in the Test Section ( $p_0 = 0.1$ MPa)

The heterogeneous O<sub>2</sub>/coal mixture was initiated with the aid of ISs using a gas mixture of C<sub>2</sub>H<sub>2</sub> + 2.5O<sub>2</sub>. To obtain stoichiometry in the volume of the TS at atmospheric pressure of oxygen, 12.77 g of carbon is required, which corresponds to a mass of coal suspension  $m \approx 16.3$  g ( $\rho \approx 726$  g/m<sup>3</sup>). The experiments were carried out at  $\rho \approx 230$ –698 g/m<sup>3</sup>,  $p_{0i} = 0.25$ –0.36 MPa, and  $w_i \approx 19.2$ –27.6 MJ/m<sup>2</sup>.

The values  $p_{0i} = 0.25$ –0.36 MPa correspond to blast wave velocities  $D_{12} \approx 1200$ –1500,  $D_{24} \approx 1116$ –1345,  $D_{34} \approx 1084$ –1247,  $D_{45} \approx 1043$ –1200,  $D_{67} \approx 851$ –1053, and  $D_{78} \approx 846$ –976 m/s. That is, blast waves in the O<sub>2</sub>/charcoal heterogeneous mixture are attenuating.



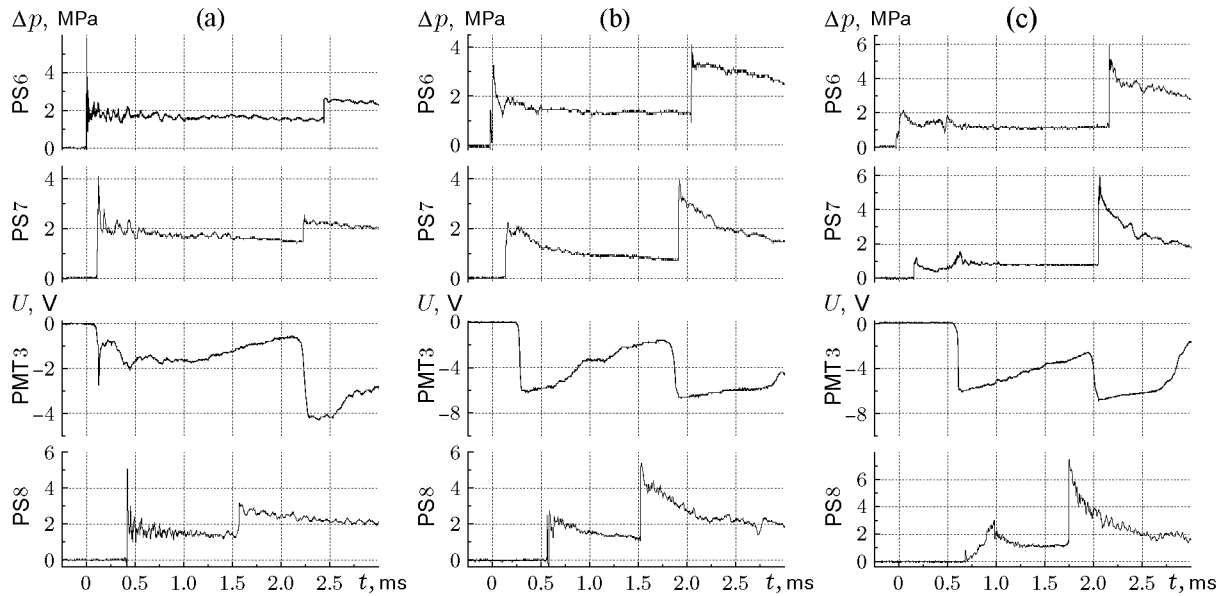


**Fig. 6.** Oscillograms of pressure and luminescence in incident detonation and reflected waves ( $p_0 = 0.1$  MPa,  $p_{0i} = 0.25$  MPa, and  $w_i \approx 19.2$  MJ/m<sup>2</sup>) for gas mixture of CH<sub>4</sub> + 2O<sub>2</sub> + 6N<sub>2</sub> (a) and hybrid mixture of (CH<sub>4</sub> + 2O<sub>2</sub> + 6N<sub>2</sub>)/coal for  $\rho \approx 180$  (b) and 515 g/m<sup>3</sup> (c).

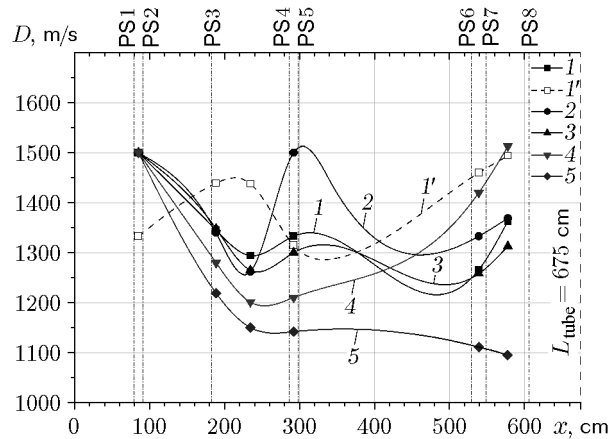


**Fig. 7.** Experimental velocities of incident DW (curves 1–5) and reflected DW (curve 1') along the tube length ( $p_0 = 0.1$  MPa,  $p_{0i} = 0.25$  MPa, and  $w_i \approx 19.2$  MJ/m<sup>2</sup>) for hybrid mixture of (CH<sub>4</sub> + 2O<sub>2</sub> + 6N<sub>2</sub>)/coal at  $\rho \approx 179$  (1 and 1'), 248 (2), 252 (3), 500 (4), and 515 g/m<sup>3</sup> (5).

In the upper half of the tube, the luminescence increases slightly after 1–1.5 ms from the blast wave front, but then, after 4–7 ms, it ceases. In this case, the luminescence time decreases with increasing suspension density. Coal dust is ignited behind the blast-wave front, and this flame propagates with an increasing lag of 1–2 m from the shock front of the blast wave. In this case, coal burning does not increase the blast wave pressure.

From PMT3 and PS8 signals, it can be established that the luminescent reaction products in the lower half of the tube ( $x \approx 5.5$  m) lag behind the leading shock front by 1–1.7 m (Fig. 8a). In the reflected wave, the beginning of luminescence practically coincides with the shock front (PMT3 and PS7 signals in Fig. 8a), and the reflected-wave velocities are  $D_{87} \approx 537$ –913 and  $D_{76} \approx 663$ –1136 m/s.

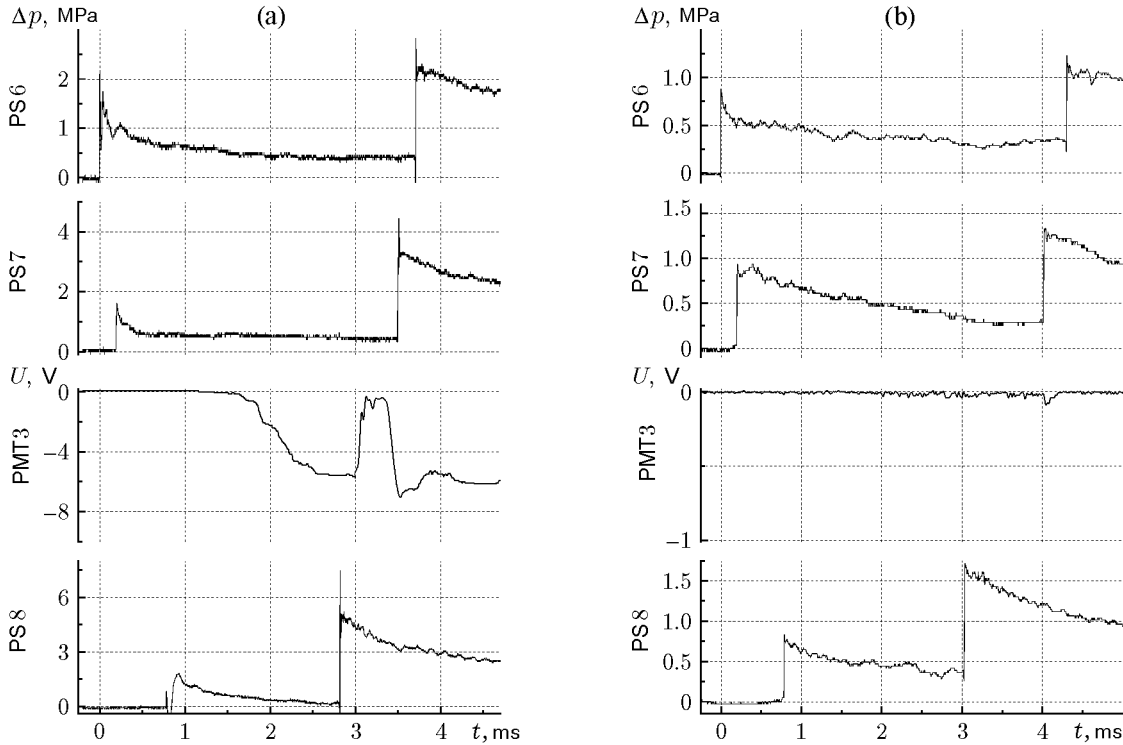


**Fig. 8.** Oscillograms of pressure and luminescence in the blast and reflected waves [ $p_0 = 0.1$  MPa,  $p_{0i} = 0.36$  MPa ( $w_i \approx 27.6$  MJ/m<sup>2</sup>): (a) O<sub>2</sub>/coal hybrid mixture ( $m \approx 7.2$  g and  $\rho \approx 275$  g/m<sup>3</sup>); (b) air.

Even with such strong initiation parameters ( $p_{0i} = 0.36$  MPa), the coal suspension reacts very weakly with oxygen behind the blast-wave front, and detonation in the heterogeneous O<sub>2</sub>/coal mixture is not initiated.

In experiments in which coal dust is absent and the TS is filled with air ( $p_0 = 0.1$  MPa,  $p_{0i} = 0.36$  MPa), the velocities of the primary (from the IS) blast wave are  $D_{12} \approx 1224$ – $1333$ ,  $D_{24} \approx 1242$ – $1246$ ,  $D_{34} \approx 1091$ – $1200$ ,  $D_{45} \approx 1203$ – $1205$ ,  $D_{67} \approx 998$ – $1003$ , and  $D_{78} \approx 975$ – $986$  m/s. The flame from the blast wave from the ISs does not reach the optical section (Fig. 8b). The velocities of the reflected shock waves are  $D_{87} \approx 575$ – $581$  and  $D_{76} \approx 697$ – $714$  m/s, about 300 m/s lower than in the O<sub>2</sub>/coal heterogeneous mixture. In the upper half of the tube, the luminescent products of gas detonation emitted from the ISs move near the blast-wave front, and their luminescence lasts 2–3 times longer (about 12.5 ms) than in the O<sub>2</sub>/coal heterogeneous mixture.

In the O<sub>2</sub>/C stoichiometric mixture for the case where carbon is in the gas and condensed phases with the percentage of the gas phase increasing from zero to stoichiometry, the calculated detonation velocity  $D_0 \approx 2050$ – $3780$  m/s [27]. The calculated temperature of detonation products corresponding to this phase frac-

tion of carbon is  $T_0 \approx 4000$ – $8700$  K. It follows from our experiments that the O<sub>2</sub>/coal mixture cannot be considered homogeneous and carbon in coal cannot be identified with carbon in the gas or condensed phase (as in [27]). The blast-wave parameters in the O<sub>2</sub>/coal heterogeneous mixture are close to those in air. The reflected-wave velocity in the heterogeneous mixture is about 300 m/s higher than in air or oxygen (no coal dust). In the reflected wave, partial combustion of the smallest particles of coal and volatiles formed behind the front of the incident blast wave is observed.

## CONCLUSIONS

1. The parameters and structure of detonation and combustion waves in fuel-lean mixtures of methane with oxygen and air and in hybrid systems consisting of a gas mixture and a fine coal suspension were experimentally determined.

2. Behind the front of combustion, blast, and detonation waves in hybrid systems, ignition and combustion of coal particles occur. An increase in the length of the reaction zone in gas mixtures leads to an increase in the degree of combustion of coal particles and an enhancement of compression waves.

3. In hybrid systems with a reactive gas mixture, steady-state detonation waves can propagate, and in hybrid systems with a less reactive gas mixture, attenuating blast waves are formed, whose parameters depend on the initiation energy.

4. In the hybrid systems studied, coal combustion competes with methane combustion, but methane is chemically more active than coal. Methane, rather than coal carbon has a decisive influence on the parameters of combustion and detonation waves.

5. In hybrid systems, the detonation parameters and the resulting heat release in the reaction zone increases insignificantly in comparison with gas mixtures, and the temperature in the reaction zone increases by no more than 15%.

6. Coal dust attenuates the detonation wave in the stoichiometric gas mixture, and low-velocity detonation propagates in the hybrid mixture. The reflection of the low-velocity detonation wave leads to the initiation of low-velocity or high-velocity detonation, depending on the degree of wave attenuation.

7. Coal suspension behind the blast-wave front weakly reacts with oxygen, and detonation in the heterogeneous O<sub>2</sub>/coal mixture is not initiated. The blast-wave parameters in the heterogeneous O<sub>2</sub>/coal mixture and in air are similar despite the ignition of the coal suspension. The reflected velocity waves in the heterogeneous mixture is about 300 m/s higher than in the gas.

8. After the passage of several additional reflected waves through the suspension, the percentage of burned coal in combustion, blast, and detonation waves exceeds 20–30%. Combustion of fine coal in combustion, blast, and detonation waves is less effective than longer-time combustion of coal in boilers and furnaces.

9. Blast and detonation processes in hybrid mixtures must be modeled taking into account the dynamics, heat transfer, ignition, and combustion individual coal particles behind the shock front. Thermodynamic calculations of detonation parameters of hybrid gas-coal systems under the assumption that carbon is in the gas and condensed phases give significantly overestimated detonation parameters in comparison with experiment.

## REFERENCES

1. W. Cybulski, *Coal Dust Explosions and Their Suppression* (Warsaw, 1976).
2. K. A. Lebetzki and S. B. Romanchenko, *Dust Explosion Hazard of Mining Production* (Gornoe Delo, Moscow, 2012); ISBN 978-5-905450-23-5.
3. A. T. Airuni, F. S. Klebanov, and O. V. Smirnov, *Explosion Hazard of Coal Mines* (Gornoe Delo, Moscow, 2012); ISBN 978-5-9950-0131-7.
4. D. Yu. Paleev, I. M. Vasenin, V. N. Kosterenko et al., *Shock Waves during Explosions in Coal Mines* (Gornoe Delo, Moscow, 2012); ISBN 978-5-905450-24-2.
5. E. V. Scholl and V. Wiemann, "Suppression of Explosions in Underground Workings Using Automatic Barriers of the BVS System," *Gluckauf-Forschungshefte*, No. 1, 38–46 (1979).
6. A. V. Dzhigrin, Yu. V. Gorlov, and V. D. Chigrin, "Automatic Explosion Suppression System—Localization of Explosions of a Methane–Air Mixture and Coal Dust in Underground Shafts of Coal Mines," *Bezopas. Tr. Prom.*, No. 8, 22–26 (2003).
7. Yu. V. Gorlov and V. I. Postnikov, "Increasing the Efficiency of Localization of Explosions of Methane–Air Mixture and Coal Dust," in *Problems of Accelerating Scientific and Technological Progress in Mining Production, Proc. of the Int. Conf.* (Lyubertsy, 2002), pp. 330–336.
8. V. V. Azatyan, "Kinetic Aspects of Chemical Methods of Preventing and Extinguishing Fires," *Zh. Vsesoyuzn. Ob. Mendeleeva*, No. 1, 4–12 (1985).
9. V. V. Azatyan, "Chemical Control of Chain Combustion is a Promising Method for Preventing Fires and Explosions of Methane–Air Mixtures," *Vestn. Nauch. Ts. Bezopas. Rabot Ugol. Prom.*, No. 2, 40–44 (2016).
10. A. V. Pinaev, A. A. Vasil'ev, and P. A. Pinaev, "Suppression of Gas Detonation by a Dust Cloud at Reduced Mixture Pressures," *Shock Waves* **25** (3), 267–275 (2015); DOI: 10.1007/s00193-014-0543-2.
11. A. V. Pinaev, A. A. Vasil'ev, and P. A. Pinaev, "Critical Parameters of a Dust Curtain Providing Complete Extinction of Gaseous Detonation Waves," *Vest. Nauch. Ts. Bezopas. Rabot Ugol. Prom.*, No. 2, 113–120 (2016).
12. M. Wolinski and P. Wolanski, "Gaseous Detonation Processes in Presence of Inert Particles," *Arch. Combust.* **7** (3/4), 353–370 (1987).
13. R. Bouchet and P. Laffite, "L'extinction des Ondes Par Les Substances Pulverisees," *C. R. Acad. Sci.* **246**, 1858–1861 (1958).
14. P. Laffite and R. Bouchet, "Suppression of Explosion Waves in Gaseous Mixtures by Means of Fine Powders," in *7th Symp. (Int.) On Combustion* (Butterworth, London, 1958), pp. 504–508.
15. C. W. Kauffmann, P. Wolanski, A. Arisoy, et al., "Dust, Hybrid and Dusty Detonation," *AIAA Progr. Astronaut. Aeronaut.* **94**, 221–239 (1984).
16. P. Wolanski, J. C. Liu, C. W. Kauffmann, et al., "The Effects of Inert Particles on Methane–Air Detonations," *Archiv. Combust.* **8** (1), 15–32 (1988).
17. Z. Chen, B. Fan, and X. Jiang, "Suppression Effects of Powder Suppressant on the Explosions of Oxyhydrogen Gas," *J. Loss Prev. Process Ind.* **19**, 648–655 (2006).

18. J. Dong, B. Fan, B. Xie, and J. Ye, "Experimental Investigation and Numerical Validation of Explosion Suppression by Inert Particles in Large-Scale Duct," *Proc. Combust. Inst.* **30**, 2361–2368 (2005).
19. A. V. Fedorov, P. A. Fomin, V. M. Fomin, D. A. Tropin, and J.-R. Chen, *Physico-Mathematical Modeling of Detonation Suppression by Clouds of Small Particles* (NGASU, Novosibirsk, 2011); ISBN 978-5-7795-0517-8.
20. A. A. Vasil'ev, V. A. Vasil'ev, A. V. Pinaev, A. V. Trotsyuk, and P. A. Fomin, "Gas-Dynamic Parameters of Combustion and Detonation of Methane–Air–Coal Dust Mixtures," in *Proc. of the XIV Minsk Int. Forum on Heat and Mass Transfer, Minsk, Belarus, September 10–13, 2012*, Vol. 2, Chapter 2, pp. 422–425.
21. A. A. Vasil'ev, A. V. Pinaev, A. V. Trotsyuk, P. A. Fomin, A. A. Trubitsyn, and D. A. Trubitsyna, "Complete Suppression of Combustion and Detonation Waves Using a Dust Curtain," *Vestn. Nauch. Ts. Bezopas. Rabot Ugol. Prom.*, No. 4, 12–21 (2015).
22. A. A. Vasil'ev, A. V. Pinaev, P. A. Fomin, A. V. Trotsyuk, V. A. Vasil'ev, A. A. Trubitsyn, and D. A. Trubitsyna, "Estimates of the Conditions of Initiation and Suppression of Blast Waves in Mine Explosions," *Vestn. Nauch. Ts. Bezopas. Rabot Ugol. Prom.*, No. 2, 91–105 (2016).
23. A. A. Vasil'ev, A. V. Pinaev, A. A. Trubitsyn, A. Yu. Grachev, A. V. Trotsyuk, P. A. Fomin, and A. V. Trilis, "What is Burning in the Mine: Methane or Coal Dust," *Fiz. Goreniya Vzryva* **53** (1), 11–18 (2017) [*Combust., Expl., Shock Waves* **53** (1), 8–14 (2017)].
24. A. V. Pinaev, "Measurement of Pressure behind a Detonation Wave Front in a Heterogeneous Gas–Film System," *Fiz. Goreniya Vzryva* **19** (1), 105–111 (1983) [*Combust., Expl., Shock Waves* **19** (1), 100–105 (1983)].
25. G. A. Lyamin, A. V. Pinaev, and A. S. Lebedev, "Piezoelectrics for Measurement of Impulsive and Static Pressures," *Fiz. Goreniya Vzryva* **27** (3), 94–103 (1991) [*Combust., Expl., Shock Waves* **27** (3), 355–363 (1991)].
26. A. V. Pinaev and G. A. Lyamin, "Piezoelectric-Pressure Transducers and Methods for Their Calibration," *Prib.Tekh. Exp.*, No. 2, 236–239 (1992).
27. A. A. Vasil'ev and V. A. Vasil'ev, "Calculated and Experimental Parameters of Combustion and Detonation of Mixtures Based on Methane and Coal Dust," *Vestn. Nauch. Ts. Bezopas. Rabot Ugol. Prom.*, No. 2, 8–39 (2016).
28. B. V. Voitsekhovskii, V. V. Mitrofanov, and M. E. Topchiyan, *Structure of the Detonation Front in Gases* (Izd. Sib. Otd. Ross. Akad. Nauk, Novosibirsk, 1963).